Hindawi Publishing Corporation
Journal of Theoretical Chemistry
Volume 2014, Article ID 125841, 10 pages
http://dx.doi.org/10.1155/2014/125841

Research Article

Normal Modes, Molecular Orbitals and Thermochemical Analyses of 2,4 and 3,4 Dichloro Substituted Phenyl-*N*-(1,3-thiazol-2-yl)acetamides: DFT Study and FTIR Spectra

Ambrish K. Srivastava,[1] Anoop K. Pandey,[1] B. Narayana,[2] B. K. Sarojini,[3] Prakash S. Nayak,[2] and Neeraj Misra[1]

[1] *Department of Physics, University of Lucknow, Lucknow, Uttar Pradesh 226007, India*
[2] *Department of Studies in Chemistry, Mangalore University, Mangalagangotri, Karnataka State 574199, India*
[3] *Department of Chemistry, P. A. College of Engineering, Mangalore, Karnataka State 574153, India*

Correspondence should be addressed to Neeraj Misra; neerajmisra11@gmail.com

Received 12 September 2013; Accepted 2 December 2013; Published 29 January 2014

Academic Editor: G. Narahari Sastry

A detailed spectroscopic analysis of two dichloro substituted phenyl-*N*-(1,3-thiazol-2-yl)acetamides at 2,4 and 3,4 positions of the phenyl ring has been carried out by using B3LYP method with 6-31+G(d, p) basis set within density functional scheme. The scaled theoretical wave numbers are in perfect agreement with the experimental values and the vibrational modes are interpreted in terms of potential energy distribution (PED). The internal coordinates are optimized repeatedly to maximize the PED contributions. The molecular HOMO-LUMO surfaces, their respective energy gaps, and MESP surfaces have also been drawn to explain the chemical activity of both molecules. Various thermodynamic parameters are presented at the same level of theory.

1. Introduction

Acetamide constitutes a distinguished class of biologically active molecules having an amide bond same as that between amino acids in proteins. Amides are also popular for their coordinating ability and which enable them to be used as ligands [1]. In general, a large number of natural products and drugs comprises of heterocyclic moieties containing nitrogen and sulphur atoms [2, 3] and interesting biological activities have been found to be associated specially with thiazole derivatives [4, 5]. In continuation to our previous studies on vibrational dynamics of biomolecules [6, 7], we intend here to report a detailed analysis of vibrational modes of molecules consisting of thiazole ring with acetamide ligand. More recently, such molecules have been shown to possess anti-HIV activities with suitable substitutions [8].

We present density functional based theoretical studies on two molecules, namely, 2-(2,4-dichlorophenyl)-*N*-(1,3-thiazol-2-yl)acetamide and 2-(3,4-dichlorophenyl)-*N*-(1,3-thiazol-2-yl)acetamide. The two molecules differ only in the position of two chlorines substituted on the phenyl ring. This provides us an opportunity to analyse the effect of position of substitution on vibrational properties. Keeping it in mind, we offer a complete assignment of all normal modes of vibration. The calculated vibrational spectra are compared with the observed ones. The chemical reactivity of molecules is also explained with the help of molecular orbital analysis. The thermochemistry of molecules is discussed by calculating various thermodynamical parameters.

2. Computational Method and FTIR Spectra

All the computations were carried out with Gaussian 09 program [9] and Chem3D Ultra 8.0 program [10] was used for a visual presentation of the graphics. The geometries of both molecules were optimized using a hybrid type B3LYP exchange-correlation functional with 6-31+G(d, p) basis set in the framework of DFT. The present computational scheme is very popular and extensively employed in the biomolecular

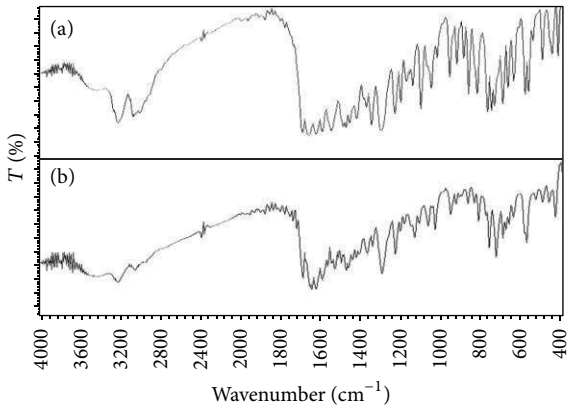

FIGURE 1: FTIR spectra of (a) 2-(2,4-dichlorophenyl)-*N*-(1,3-thiazol-2-yl)acetamide and (b) 2-(3,4-dichlorophenyl)-*N*-(1,3-thiazol-2-yl)acetamide recorded with samples in KBr pallet.

studies due to reliability of its results as compared to experimental data [11]. Vibrational analyses of molecules were performed at the same level of theory. The normal mode frequencies were scaled by equation, $\nu_{\text{scaled}} = 22.1 + 0.9543\nu_{\text{calculated}}$ as recommended by many studies [12–14] in order to make comparison with the observed wavenumbers.

To perform experimental FTIR spectroscopy, the title compounds were purchased from Sigma Aldrich with a purity of 98% and used as such without further purification for spectroscopic processing. The FTIR spectra were recorded by using Shimadzu-Model Prestige 21 spectrometer in the region 400–4000 cm^{-1} with samples in KBr pellet. The FTIR spectra of title molecules are shown in Figure 1.

3. Results and Discussions

3.1. Crystal Structure and Molecular Geometry. We have already reported X-ray crystallographic studies on these compounds [15, 16]. All these compounds belong to triclinic $P\bar{1}$ space group. In crystal phase, molecules are linked by pairs of N–H$\cdots$N hydrogen bonds. There is also a weak C–H$\cdots$O interaction in case of 2,4 substitution.

The crystallographic parameters were used to model initial structure for the process of geometry optimization. The optimized geometries of both molecules are displayed in Figure 2. The mean plane of dichlorophenyl ring is almost perpendicular to that of thiazole ring in both molecules thus forming a sofa shaped structure. The angular changes in hexagonal ring geometry have also been proven to be a sensitive indicator of the interaction between the substituent and the ring [17]. The structural changes in the carbon skeleton involve changes in the bond distances as well as bond angles. They are most pronounced at the place of substitution and depend on the electronegativity as well as on the σ/π, donor/acceptor character of the substituent. All bond-lengths and bond angles are nearly same in both molecules except those in phenyl ring attached with chlorine atoms at different positions. For instance, C–Cl, bond-length 1.752–1.756 Å in 2,4 substituted molecule is reduced to 1.744-1.745 Å for 3,4 substitution.

In Figure 3, we have shown a linear correlation between DFT calculated and X-ray experimental bond-lengths for title molecules. Note that C–H bond-lengths are not included here. A correlation coefficient (R^2) of greater than 0.99 in both molecules supports the fact that DFT can efficiently reproduce the experimental geometry.

3.2. Normal Mode Analysis. The calculated IR and observed FTIR spectra of both molecules are shown in Figure 4 for comparison in the wavenumber range of 1800–400 cm^{-1}. The calculated wavenumbers are scaled by using the equation mentioned earlier. All the vibrational modes were properly assigned on the basis of the potential energy distribution (PED). Tables 1 and 2 list calculated frequencies (unscaled as well as scaled), FTIR observed frequencies, IR intensities, and assignments of all normal modes for title molecules. Both molecules contain two ring system, a phenyl ring (R1) and a thiazole ring (R2) connected by acetamide fragment (–NHCOCH$_2$–). For the clarity of discussions, we classified their vibrations into three broad categories.

3.2.1. Phenyl Ring (R1) Vibrations. The phenyl ring vibrations contain the C–H stretching modes in the region 3100–3000 cm^{-1}, which is the characteristic region for the identification of C–H stretching vibrational modes [18]. In this region, the bands are not much affected by the nature of the substituents. The scaled C–H modes are found between 3096–3060 cm^{-1} which are observed at 3055 cm^{-1} for 2,4 substituted molecule polarized along 3C–6C and at 3034 cm^{-1} for 3,4 substitution. These modes are purely stretching having PED greater than 90%. Most of the C–H stretching modes are found to be weak due to charge transfer from hydrogen to carbon atom. Other C–H modes coming from bending (in-plane and out-of-plane), breathing and twisting of ring are found in the region below 1500 cm^{-1} having medium to weak intensities.

The C–C ring stretching vibrations are expected within the region 1650–1200 cm^{-1} [19]. Most of these ring modes are affected by the substitution to aromatic ring. Scaled frequencies for C–C stretching modes at B3LYP/6-31+G(d, p) are 1580 cm^{-1}, 1548 cm^{-1}, and 1477 cm^{-1} for 2,4 and 1583 cm^{-1}, 1549 cm^{-1}, and 1476 cm^{-1} for 3,4 substitution on the ring. Some other C–C modes associated with bending, twisting and breathing vibrations are also found to lie in lower frequency region as well as overlapped with other modes. Most of C–C modes are comparatively stronger than C–H modes.

3.2.2. Thiazol Ring (R2) Vibrations. The vibrations of thiazole ring associated with C–H stretching are calculated in between 3145–2950 cm^{-1} for title molecules which are essentially independent on the substitutions in the phenyl ring. These values are in agreement with observed bands in thiazoles and its derivatives [20]. The most intense bands corresponding to C–N stretching in thiazole are calculated at 1532-1531 cm^{-1}.

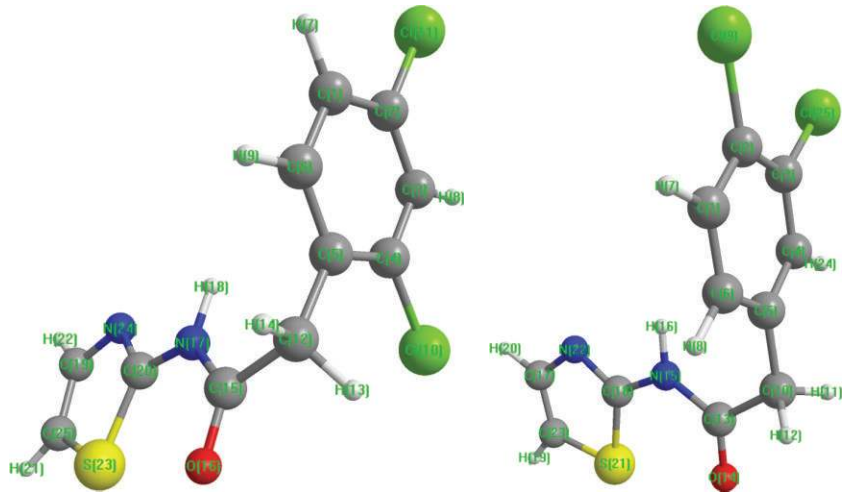

(a) (b)

FIGURE 2: Optimized geometries of (a) 2-(2,4-dichlorophenyl)-*N*-(1,3-thiazol-2-yl)acetamide and (b) 2-(3,4-dichlorophenyl)-*N*-(1,3-thiazol-2-yl)acetamide corresponding to the global minima calculated at B3LYP/6-31+G(d, p) level.

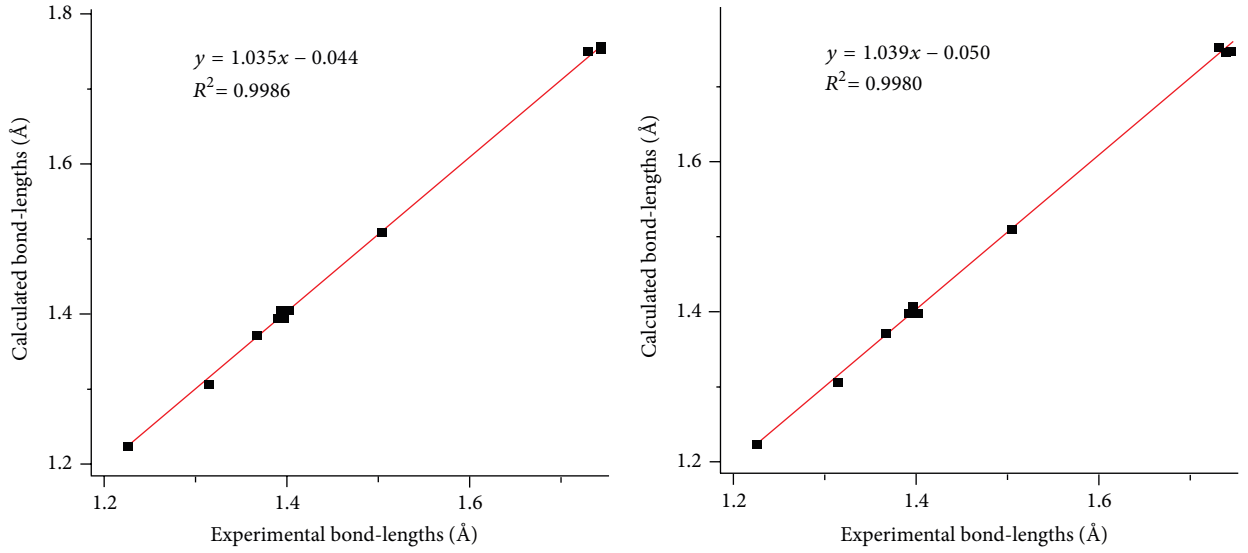

(a) (b)

FIGURE 3: Correlation between X-ray experimental and DFT calculated bond-lengths for (a) 2-(2,4-dichlorophenyl)-*N*-(1,3-thiazol-2-yl)acetamide and (b) 2-(3,4-dichlorophenyl)-*N*-(1,3-thiazol-2-yl)acetamide.

These vibrational modes are found to be coupled with N–H stretching and polarized along phenyl ring. The same bands are observed at 1544 cm^{-1}–1527 cm^{-1} in the FTIR spectra. Other weak modes of thiazole ring vibration associated with breathing and twisting of rings are calculated below 1500 cm^{-1} and those specially associated with S atom are found near 600 cm^{-1}.

3.2.3. Fragment (–NHCOCH$_2$–) Vibrations. Amides show somewhat strong and broad band in the range between 3500 cm^{-1} and 3100 cm^{-1} for N–H stretch as well as a stronger band between 1700 cm^{-1} and 1650 cm^{-1} for C=O stretching [21]. Carbonyl absorptions are very sensitive and both the carbon and the oxygen atoms move during the vibration having nearly equal amplitude. The scaled values, 3458 cm^{-1}–3456 cm^{-1} for N–H stretch and 1690 cm^{-1}–1685 cm^{-1} for C=O stretch agree with literature values. In FTIR spectra, the corresponding band for C=O stretching are observed at 1691 cm^{-1}–1689 cm^{-1} while N-stretching frequencies are lowered to 3199 cm^{-1}–3197 cm^{-1}. The differences between calculated and observed N–H stretch band are attributed to the presence of intermolecular H-bond in condensed phase which are absent in the isolated state of molecules.

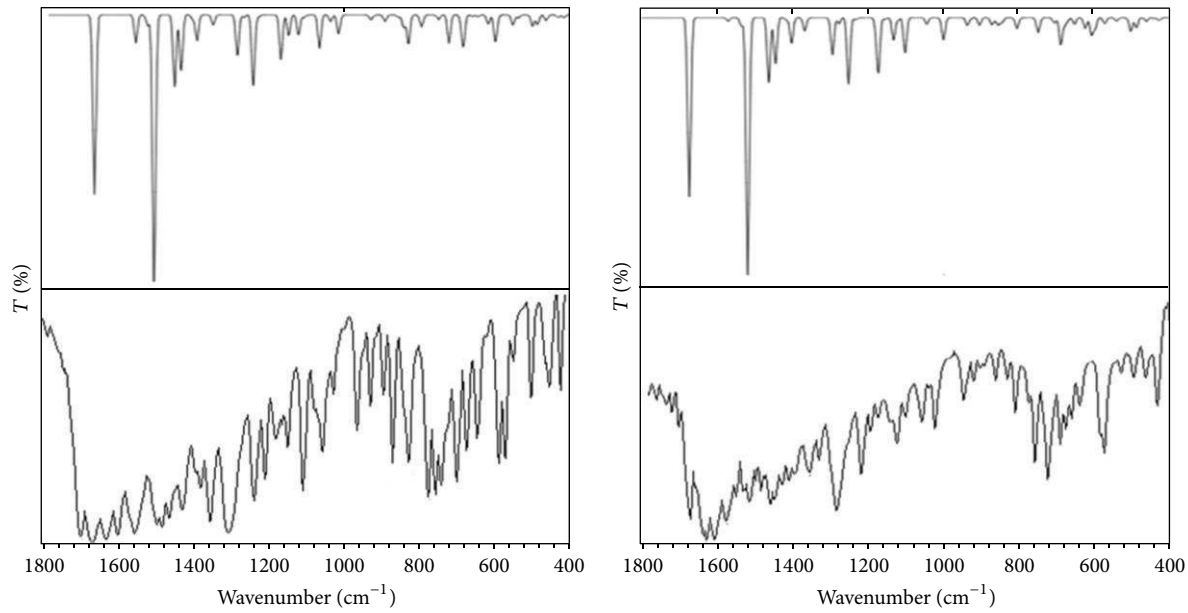

Figure 4: Calculated IR and observed FTIR spectra of (a) 2-(2,4-dichlorophenyl)-*N*-(1,3-thiazol-2-yl)acetamide and (b) 2-(3,4-dichlorophenyl)-*N*-(1,3-thiazol-2-yl)acetamide for comparison in the frequency range of 1800 cm^{-1}–400 cm^{-1}.

In acetamide fragment, the stretching of methylene ($-CH_2$) group and bending (scissoring and rocking) always occur in 3000 cm^{-1}–2850 cm^{-1} and below 1500 cm^{-1}, respectively [20]. These vibrations are more common and so are not much of significance. The stretching mode polarized along to ring R2 corresponding to $-CH_2$ is calculated at 2950 cm^{-1} for 2,4 substitution and 2947 cm^{-1} for 3,4 substituted molecule.

3.3. Molecular Orbital Analysis. The highest occupied molecular orbital (HOMO) represents ability to donate an electron while lowest unoccupied molecular orbital (LUMO) denotes ability to accept it. The HOMO-LUMO plots for title molecules are shown in Figure 5. Evidently, the HOMOs of both molecules are located on the thiazole ring including amide fragment while the LUMOs are contributed mainly by phenyl ring system. The transition from HOMO → LUMO in these molecules indicates charge transfer to phenyl ring. The energy difference (E_{gap}) between HOMO and LUMO describes the chemical reactivity of molecule. The smaller E_{gap}, 4.89 eV in 2,4 substituted molecule as compared to 4.94 eV in 3,4 substitution may suggest that former is chemically more reactive than the latter one. The chlorine atoms attached to adjacent carbons on phenyl ring for 3,4 substituted molecule make it less reactive.

Figure 5 also plots the molecular electrostatic potential (MESP) surface for title molecules. The MESP, a map of electrostatic potential on uniform electron density, is used to visualize charge or electron density distribution within the molecule. The importance of MESP lies in the fact that it simultaneously displays molecular size, shape as well as positive, negative, and neutral electrostatic potential regions in terms of colour grading. In present context, colour code varies between positive region for red and negative for blue regions with an isovalue of 1.00000 eV. Evidently, the electronegative region lies in the vicinity of carbonyl group of amide fragment. On the basis of MESP plot, it can be asserted that an electrophile will be attracted towards the negative region of amide fragment in both molecules.

3.4. Thermochemical Analysis. Thermochemical properties of molecules are dominated by molecular vibrations as electronic contribution becomes negligible due to absence of free electrons, especially at the room temperature. Various thermal parameters for title molecules are calculated and reported in Table 3. These parameters are related to one another via standard thermodynamic relations and can be useful for the estimation of chemical reaction paths. Zero point energy (ZPE) is also given. Thermal energy of 3,4 substituted molecule is slightly higher than that with 2,4 substitution while heat capacity is smaller. The entropy values are closely related to the geometry of molecules. The substitution of chlorines at 3,4 position of ring leads to an increase in entropy value as compared to 2,4 substitution. The increase in thermal energy and entropy values may indicate the enhancement in molecular vibrations due to steric repulsion generated with chlorine atoms substituted at two consecutive (3,4) positions of the phenyl ring.

4. Conclusions

We have performed a theoretical density functional calculations on dichloro substituted phenyl-*N*-(1,3-thiazol-2-yl)acetamides at 2,4 and 3,4 positions of the phenyl ring. The calculated structural parameter shows a good correlation

Table 1: Normal mode assignments of 2-(2,4-dichlorophenyl)-*N*-(1,3-thiazol-2-yl)acetamide at B3LYP/6-31+G (d,p) level.

S.number	Unscaled freq. (cm^{-1})	Scaled freq. (cm^{-1})	FTIR freq. (intensity) (cm^{-1})	IR intensity (a.u.)	Mode of vibration (%PED)	Direction of polarization
1	3600	3458	3199 (s)	79	ν(N17–18H) (100)	Along N–H plane
2	3272	3145		1	ν(C–H)R2 (99)	Along R1
3	3243	3117		1	ν(C–H)R2 (99)	Along R2
4	3234	3108		8	ν_{as}(22H–19C–25C–21H) (89)	Per R2
5	3226	3101		1	ν(C–H)R1 (99)	Along R2
6	3188	3064	3055 (w)	5	ν(C–H)R1 (98)	Along to 3C–6C
7	3121	3001		1	ν_{as}(22H–19C–25C–21H) (89)	Along R2
8	3068	2950		7	ν(13H–12C–14H) (91)	Along R2
9	1748	1690	1691 (s)	273	ν(15C–16O) (83)	Opposite to C–O
10	1632	1580		42	ν(C–C)R1 (59)	Along R2
11	1599	1548	1544 (m)	16	ν(C–C)R1 (65) + β(C–H)R1(14)	Along 6C–9H
12	1581	1531		420	ν(20C–24N) (55) + β(17N–18H) (21)	Along R1
13	1524	1477		109	ν(19C–25C) (54) + β(17N–18H) (12) + β(C–H)R2 (15)	Per R2
14	1506	1459		84	β(C–H)R1 (74)	Along R2
15	1473	1428		6	Scissoring (13H–12C–14H (55)) + ν(20C–24N) (40)	Along R2
16	1461	1416		38	Scissoring (13H–12C–14H) (72) + β(17N–18H) (15)	Per R2
17	1416	1373	1346 (m)	15	ν(C–C)R1 (30) + β(C–H)R1 (27)	Along R2
18	1348	1308		61	β(C–H)R1 (86)	Along 19C–22H
19	1339	1300	1300 (vw)	1	Rocking (13H–12C–14H)(39) + β(C–H)R2 (42)	Along R2
20	1330	1291		3	Rocking (13H–12C–14H) (30) + ν(C–C)R2 (54)	Along R1
21	1304	1267		107	ν(20C–24N) (45) + β(17N–18H) (15)	Per R2
22	1291	1254	1230 (w)	3	β(C–H)R1 (76)	Along R2
23	1227	1193		64	β(C–H)R1 (54)+ β(17N–18H) (32)	Along R2
24	1224	1190		3	β(C–H)R1 (71)	Per R2
25	1205	1172		31	Twist (13H–12C–14H) + β(C–H)R2 and R1	Per R2
26	1178	1146		30	β(19C–22H) (65) + β(17N–18H) (15)	Along R2
27	1163	1132		4	β(1C–7H–6C–9H) (65)	Per R2
28	1119	1090	1103 (m)	50	β(3C–8H) (43) + β(6C–9H) (32)	Along R2
29	1088	1060		10	Scissoring (21H–25C–19C–22H) (56)	Along R2
30	1066	1039		28	Breathing R2	Per R1
31	976	954	960 (w)	7	Twist (13H–12C–14H) + *S*(16O–15C–17H)	Along R1
32	967	945		1	Twist (1C–7H–6C–9H)	Along R2
33	936	915		9	Rocking (13H–12C–14H) (45)	Along R2
34	898	879		3	Twist (21C–25H–19C–22H)	Per R2
35	885	867	866 (w)	11	γ(3C–8H) (49)	
36	882	864		7	Breathing R2	Along R1
37	871	853		43	Breathing R1	In between R1 and R2
38	834	818	823 (m)	18	γ(1C–7H) (44) + γ(6C–9H) (11)	Along R1

Table 1: Continued.

S.number	Unscaled freq. (cm^{-1})	Scaled freq. (cm^{-1})	FTIR freq. (intensity) (cm^{-1})	IR intensity (a.u.)	Mode of vibration (%PED)	Direction of polarization
39	786	772	771 (w)	7	γ(1C–7H) + γ(6C–9H) + β(R1)	Along C–O
40	758	746		43	β(R2)	
41	723	712		11	Ring R2 twist	Per R2
42	717	706	698 (m)	43	γ(21C–25H) (38) + γ(19C–22H) (12)	Along R2
43	693	683		2	Ring R2 twist	Along R1
44	677	668		2	T(13H–12C–14H)	
45	648	641		2	γ(C–H)R1 (54)	Directed CH_2
46	628	621		36	γ(C–H)R1 + γR2 + rocking (13H–12C–14H)	Per R2
47	623	617		7	Twist R2 + rocking (13H–12C–14H)	Along R2
48	579	575		15	γ(7C–1H) (43)+ γ(3C–8H) (39) + γ(2C–11Cl) (11)	Along 2C–11Cl
49	564	560		4	Rocking (13H–12C–14H) (23) + γ(19C–22H) (35) + γ(17N–18H) (21)	Along R1
50	524	522		16	R2 breathing + R1 twist	Per R2
51	510	509		14	γ(17C–18H) + γ(ring R2)	(Along Cl) R1
52	486	486		8	Ring R2 twist + γ(17C–18H) + γ(23C–25C–20C)	
53	452	453		3	γ(3C–8H) (35) + γ(6C–9H) (22) + R(13H–12C–14H) (31)	Along 17N–18H
54	437	439		3	Rocking (13H–12C–14H (29)) + γ(3C–8H) (35) + γ(5C–9H) (12)	Per R2
55	398	402		3	β(R1ring)	Per 17N–18H
56	357	363		1	β(C–C)R2 (23) + β(15C–16O) (34)	Along R2
57	321	328		1	γ(C–C)R2 (26) + rocking (13H–12C–14H) (17)	Along CH_2
58	298	307		1	γ(23C–21H) + γ(28C–17H) + rocking (13H–12C–14H)	Along R1
59	286	295		6	γ(ring R2)	Per R2
60	267	277		4	β(11C–2Cl) (18) + β(4C–10Cl) (13) + rocking (13H–12C–14H) (21)	Along R2
61	201	214		1	β(11C–2Cl) (11) + β(4C–10Cl) (27) + β(1C–7H) (23)	Along R2
62	174	188		1	τ(ring R1 and R2)	Per R2
63	137	153		6	γ(ring R1)	Per R2
64	105	122		1	γ(ring R2)	Per R1
65	96	114		1	γ(ring R2)	Along R2
66	77	96		4	τ(13H–12C–14H)	Per R2
67	32	53		1	Rings R1 and R2 twist jointly	Along R1
68	23	44		1	Rings R1 and R2 twist jointly	Along 4C–10Cl
69	19	40		1	Rings R1 and R2 twist jointly	Along R2

ν: stretching; ν_s: symmetric stretching; ν_{as}: asymmetric stretching; β: in-plane-bending; γ: out-of-plane bending; ω: wagging; τ: torsion, S: scissoring; vs: very strong; s: strong; m: medium; w: weak; vw: very weak.

Table 2: Normal mode assignments of 2-(3,4-dichlorophenyl)-*N*-(1,3-thiazol-2-yl)acetamide at B3LYP/6-31+G(d, p) level.

S.number	Unscaled Freq. (cm^{-1})	Scaled freq. (cm^{-1})	FTIR freq. (intensity) (cm^{-1})	IR intensity (a.u.)	Mode of vibration (%PED)	Direction of polarization
1	3598	3456	3197 (s)	97	ν(15N–16H) (100)	Along 15N–16H plane
2	3271	3144		1	ν(23C–19H) (44) + ν(17C–20H) (45)	Along 2C–9Cl
3	3234	3108		8	ν(23C–19H) (99)	Along 6C–8H
4	3220	3095		1	ν(1C–7H) + ν(6C–8H)	Along 2C–Cl
5	3204	3080		1	ν(9C–23H) (99)	Along R2
6	3191	3067	3034 (w)	4	ν(6C–8H) (48) + ν(1C–7H) (55)	Along 3C–6C
7	3106	2986		1	ν_{as}(12H–110C–11H) (89)	Along R2
8	3065	2947		8	ν(12H–10C–11H) (91)	Along R1
9	1743	1685	1689 (vs)	289	ν(15C–16O) (83)	Along 13C–14O
10	1636	1583	1589 (w)	5	ν(C–C)R1 (59)	Along R2
11	1600	1549		13	ν(C-C)R1 (65) + β(C–H)R1 (14)	Along 5C–H
12	1582	1532	1527 (vs)	461	ν(18C–22N) (55) + β(15N–16H) (21)	Per R1
13	1524	1476		104	ν(C–C)R2 (54) + β(15N–16H) (12) + β(17C–20H) (15)	Per R2
14	1506	1459	1462 (s)	74	β(C–H)R2 (74) + ν(C–C)R2 (21)	Along R2
15	1476	1431		3	Scissoring (13H–12C–14H (55)) + ν(C-N)R2 (40)	Along R2
16	1461	1416		38	Scissoring (13H–12C–14H) (72) + β(17N–18H) (15)	Along 4C–5C
17	1425	1382		41	ν(C–C)R1 (30) + β(C–H)R1 (27)	Along13C–15N
18	1349	1310		59	β(C–H)R1 (46) + ν(C–C)R1 (30)	Along R2
19	1331	1292	1294 (w)	9	Rocking (13H–12C–14H) (39) + β(C–H)R1 (42)	Along R1
20	1328	1289		1	Rocking (13H–12C–14H) (39) + ν(C–C)R1 (32)	Per R1
21	1304	1267		107	β(15C–16H) (26) + ν(C–C)R1 (54)	Per R1
22	1285	1248	1228 (w)	3	β(C–H)R1 (76)	Along R2
23	1228	1194		15	β(17C–20H) (19) + rocking (11H–10C–12H) (22) + β(C–H)R1 (26)	Making 5C–10C with an angle 45°
24	1222	1188		3	β(17C–20H) (19)+ β(15N–16H) (22) + β(4C–24H)R1 (26)	Per R2
25	1204	1171		2	Twist (11H–10C–12H) + β(6C–8H)	Per R1
26	1180	1148		35	β(17C–18H)R (65) + β(17N–18H) (15)	Along R2
27	1168	1137		3	β(1C–7H) (65) + β(6C–8H) (14)	Plane containing 13C and per to plane of R1
28	1148	1118		50	β(C–C)R1 (43) + β(C–H)R1 (32)	Along 15N–16H
29	1089	1061		10	β(17C–20H) (43) + β(23C–10H) (32)	Along R2
30	1043	1017		35	β(C–H)R1 (28) + β(C–C)R1	Per R1
31	977	955		7	Twist (13H–12C–14H) + scissoring (16O–15C–17H)	Along R1
32	970	948		1	Twist (7C–1H-6C–8H) (59)	Along R2
33	943	922		12	Rocking (13H–12C–14H) (45) + γ(4C–24H) (29)	Along R2
34	909	890		11	γ(C–H) (23) + γ(C–C) (49)	Per R2
35	898	879		3	γ(C–H)R2 (49)	Per R2
36	891	872		10	Breathing R1+ γ(4C–24H)	Along 6C–5H
37	881	863		7	Breathing R2	Along 15N–10H

Table 2: Continued.

S.number	Unscaled Freq. (cm^{-1})	Scaled freq. (cm^{-1})	FTIR freq. (intensity) (cm^{-1})	IR intensity (a.u.)	Mode of vibration (%PED)	Direction of polarization
38	840	824	815 (m)	17	γ(6C–8H) (44) + γ(1C–7H) (11)	Along R1
39	781	767	763 (m)	23	γ(6C–8H) + β(ring R1)	Along C–O
40	737	725	729 (w)	8	γ(C–C)R1 (44) + γ(C–H)R1 (11)	
41	719	708		43	γ(23C–14H) (32) + γ(17C–20H) (53)	Per R2
42	708	698		11	γ(C–C) (38) + rocking (11–10C–12H) (12)	Along R2
43	699	689		3	γ(C–H) (23) + γ(C–C) (49)	Along 13–14O
44	681	672		10	τ(13H–12C–14H)	
45	652	644		17	γ(C–S–C)R2 (54)	Directed CH_2
46	634	627		27	γ(15C–16H)R2 + γR2 + rocking (11H–10C–12H)	Per R2
47	624	618		17	γ(C–S–C)R2 (43) + γ(C–H)R2 (39)	Along R2
48	598	593	580 (w)	9	Twist R1 + Rocking (13H–12C–14H)	Per R2
49	566	562		5	γ(R2) + γ(15N–16H)	Along R1
50	526	524		21	R1 breathing + R2 twist	Per R2
51	510	509		14	γ(17C–18H) + ring R2 out-of-plane bending	Along R1
52	483	483		6	γ(CCC)R1+ γ(C–Cl)R1	Along 13C–10O
53	460	461		1	Ring R1 twist	Along 5C–4C
54	448	450		4	γ(CCC)R1 (34) + γ(1C–7H) (54)	Plane containing 16H
55	386	391		1	τ(ring R1)	Along 5C–4C
56	356	362		1	β(C–C)R1 (23) + β(15N–16H) (34)	Along R2
57	319	327		3	γ(C–C)R1 (26) + β(13C–14) (25)	Along CH_2
58	295	304		1	γ(ring R2)	Along 4C–24H
59	288	297		3	γ(CCC)R1 + γ(C–H)R1	Along 18C–15N
60	243	254		1	τ(11H–10C–12H)	Along R2
61	199	212		1	β(C–Cl)R1 (11) + β(1C–7H) (23)	Along R1
62	183	197		2	τ(ring R1)	Per R2
63	135	151		5	τ(CCC) + γ(CH)R1	Per R2
64	105	122		1	τ(ring R1)	Per R2
65	94	112		0	τ(ring R2)	Per R1
66	76	95		6	τ(11H–10C–12H) + γ(13C–14H)	Along R2
67	33	54		1	τ(ring R1)	Per R2
68	16	37		1	γ(R1)	Along R1
69	12	34		1	Rings R1 and R2 twist jointly	Along 4C–10Cl

ν: stretching; ν_s: symmetric stretching; ν_{as}: asymmetric stretching; β: in-plane-bending; γ: out-of-plane bending; ω: wagging; τ: torsion, S: scissoring; vs: very strong; s: strong; m: medium; w: weak; vw: very weak.

with corresponding experimental data showing the validity of calculations. We have presented complete vibrational mode assignments using same computational scheme. Normal modes are discussed in detail and compared with those observed by FTIR spectroscopy. The chemical reactivity of molecules is discussed by HOMO-LUMO as well as MESP analysis thus exploring the effect of substituent positions. Calculated various thermodynamic parameters are very useful in determining chemical reaction paths.

Conflict of Interests

The authors declare that there is no conflict of interests regarding the publication of this paper.

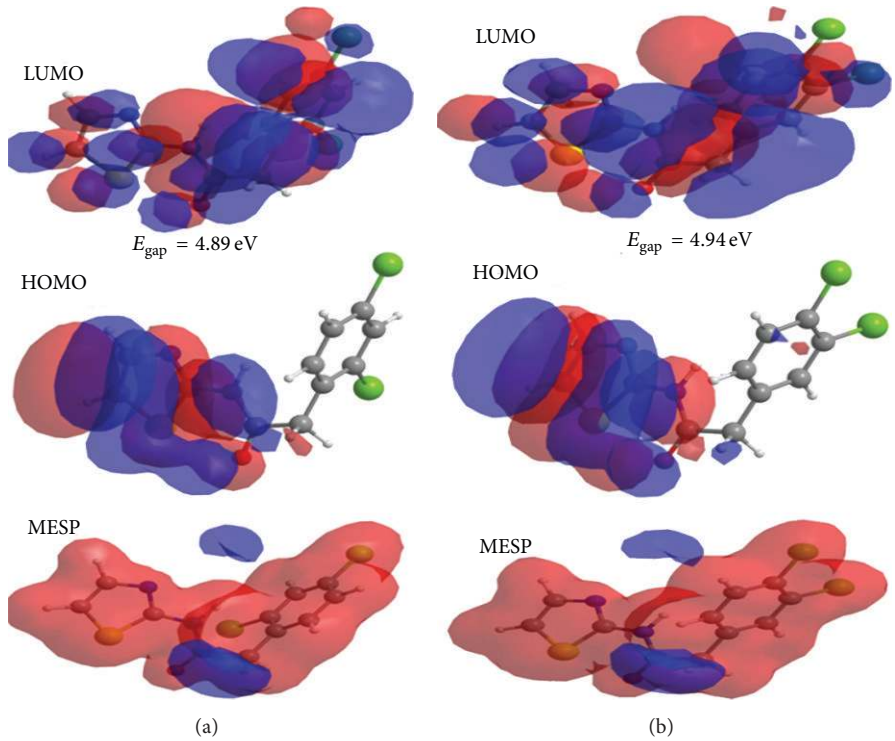

Figure 5: HOMO-LUMO and MESP plots for (a) 2-(2,4-dichlorophenyl)-*N*-(1,3-thiazol-2-yl)acetamide and (b) 2-(3,4-dichlorophenyl)-*N*-(1,3-thiazol-2-yl)acetamide.

Table 3: Total energy and various thermodynamic parameters for title molecules calculated at B3LYP/6-31+G(d,p) level.

Parameters	2-(2,4-Dichlorophenyl)-*N*-(1,3-thiazol-2-yl)acetamide	2-(3,4-Dichlorophenyl)-*N*-(1,3-thiazol-2-yl)acetamide
Electronic energy (Hartree)	−1927.348	−1927.345
ZPE (kcal/mol)	108.137	108.118
Thermal energy (kcal/mol)	117.690	117.696
Thermal enthalpy (kcal/mol)	118.281	118.287
Thermal free energy (kcal/mol)	79.187	78.675
Constant volume heat capacity (cal/mol-K)	56.509	56.438
Entropy (cal/mol-K)	131.123	132.861

Acknowledgment

Ambrish K. Srivastava gratefully acknowledge the Council of Scientific and Industrial Research (CSIR), India, for providing financial assistance in the form of Junior Research Fellowship.

References

[1] W. N. Wu, F. X. Cheng, L. Yan, and N. Tang, "Synthesis, characterization and fluorescent properties of lanthanide complexes with two aryl amide ligands," *Journal of Coordination Chemistry*, vol. 61, pp. 2207–2215, 2008.

[2] B. C. C. Cantello, M. A. Cawthorne, G. P. Cottam et al., "[[ω-(heterocyclylamino)alkoxy]benzyl]-2,4-thiazolidinediones as potent antihyperglycemic agents," *Journal of Medicinal Chemistry*, vol. 37, no. 23, pp. 3977–3985, 1994.

[3] G. Kucukguzel, A. Kocatepe, E. D. Clercq, F. Sahin, and M. Gulluce, "Synthesis and biological activity of 4-thiazolidinones, thiosemicarbazides derived from diflunisal hydrazide," *European Journal of Medicinal Chemistry*, vol. 41, no. 3, pp. 353–359, 2006.

[4] J. Quiroga, P. Hernandez, B. R. Insuassty et al., "Control of the reaction between 2-aminobenzothiazoles and Mannich bases. Synthesis of pyrido[2,1-b][1,3]benzothiazoles versus [1,3]benzothiazolo[2,3-b]quinazolines," *Journal of the Chemical Society, Perkin Transactions*, vol. 1, pp. 555–559, 2002.

[5] I. Hutchinson, S. A. Jennings, B. R. Vishnuvajjala, A. D. Westwell, and M. F. G. Stevens, "Antitumor benzothiazoles. 16. Synthesis and pharmaceutical properties of antitumor 2-(4-aminophenyl)benzothiazole amino acid prodrugs," *Journal of Medicinal Chemistry*, vol. 45, no. 3, pp. 744–747, 2002.

[6] A. K. Pandey, S. A. Siddiqui, A. Dwivedi, N. Misra, and K. Raj, "Density functional theory study on the molecular structure of loganin," *Spectroscopy*, vol. 25, no. 6, pp. 287–302, 2011.

[7] A. Dwivedi, A. K. Pandey, and N. Misra, "Vibrational analysis and electronic properties of 2-Decenoic acid and its derivative by first principles," *Spectroscopy*, vol. 26, no. 6, pp. 367–385, 2011.

[8] M. Oftadeh, N. M. Mahani, and M. Hamadanian, "Density Functional Theory Study of the Local Molecular Properties of Acetamide Derivatives as Anti-HIV Drugs," *Research in Pharmaceutical Sciences*, vol. 8, pp. 285–297, 2013.

[9] M. J. Frisch, G. W. Trucks, H. B. Schlegel et al., *Gaussian 09*, Revision B.1, Gaussian, Wallingford, UK, 2010.

[10] Chem3D Ultra, "version 8.0.3," 2003, http://www.cambridgesoft.com/.

[11] E. Taşal, İ. Sıdıra, Y. Gülseven, C. Öğretir, and T. Önkol, "Vibrational spectra and molecular structure of 3-(piperidine-1-yl-methyl)-1,3-benzoxazol-2(3H)-one molecule by density functional theory and Hartree-Fock calculations," *Journal of Molecular Structure*, vol. 923, pp. 141–152, 2009.

[12] M. A. Palafox and V. K. Rastogi, "Quantum chemical predictions of the vibrational spectra of polyatomic molecules. The uracil molecule and two derivatives," *Spectrochimica Acta A*, vol. 58, no. 3, pp. 411–440, 2002.

[13] M. A. Palafox, "Scaling factors for the prediction of vibrational spectra. I. Benzene molecule," *International Journal of Quantum Chemistry*, vol. 77, no. 3, pp. 661–684, 2000.

[14] M. A. Palafox, J. L. Núez, and M. Gil, "Accurate scaling of the vibrational spectra of aniline and several derivatives," *Journal of Molecular Structure*, vol. 593, pp. 101–131, 2002.

[15] P. S. Nayak, B. Narayana, H. S. Yathirajan, J. P. Jasinski, J. Ray, and R. J. Butcher, "2-(2,4-Dichlorophenyl)-N-(1,3-thiazol-2-yl)acetamide," *Acta Crystallographica E*, vol. 69, pp. o656–o657, 2013.

[16] P. S. Nayak, B. Narayana, H. S. Yathirajan, J. P. Jasinski, J. Ray, and R. J. Butcher, "2-(3,4-Dichlorophenyl)-N-(1,3-thiazol-2-yl)acetamide," *Acta Crystallographica E*, vol. 69, pp. o645–o646, 2013.

[17] A. Kovacs and I. Hargittai, "Theoretical investigation of the additivity of structural substituent effects in benzene derivatives," *Structural Chemistry*, vol. 11, no. 2-3, pp. 193–201, 2000.

[18] V. K. Rastogi, M. A. Palafox, R. P. Tanwar, and L. Mittal, "3,5-difluorobenzonitrile: ab initio calculations, FTIR and Raman spectra," *Spectrochimica Acta A*, vol. 58, no. 9, pp. 1987–2004, 2002.

[19] A. J. Barnes, M. A. Majid, M. A. Stuckey, P. Gregory, and C. V. Stead, "The resonance Raman spectra of Orange II and Para Red: molecular structure and vibrational assignment," *Spectrochimica Acta A*, vol. 41, no. 4, pp. 629–635, 1985.

[20] A. Taurins, J. G. E. Fenyes, and R. N. Jones, "Thiazoles: iii. Infrared spectra of methylthiazoles," *Canadian Journal of Chemistry*, vol. 35, no. 5, pp. 423–427, 1957.

[21] M. Silverstein, G. C. Basseler, and C. Morill, *Spectrometric Identification of Organic Compounds*, John Wiley & Sons, New York, NY, USA, 1981.